

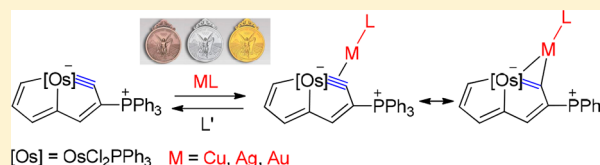
## Reactions of Cyclic Osmacarbonyne with Coinage Metal Complexes

Xiaoxi Zhou,<sup>1b</sup> Yunlong Li, Yifan Shao, Yuhui Hua, Hong Zhang,<sup>1b</sup> Yu-Mei Lin,<sup>\*1b</sup> and Haiping Xia<sup>\*1b</sup>

State Key Laboratory of Physical Chemistry of Solid Surfaces and Collaborative Innovation Center of Chemistry for Energy Materials (iChEM), College of Chemistry and Chemical Engineering, Xiamen University, Xiamen 361005, China

## Supporting Information

**ABSTRACT:** The reactions of the five-membered cyclic osmacarbonyne complex, i.e., osmapentalynes, with a complete set of coinage metal (Cu, Ag, and Au) complexes have been investigated. Osmapentalynes **1** reacts with CuCl or AuCl(PPh<sub>3</sub>) via its metal–carbon triple bond, leading to the formation of osmapentalynes–copper(I) chloride adduct **2** or osmapentalynes–gold(I)–triphenylphosphine adduct **3**, respectively. Moreover, it can react with AgOTf in the presence of 1,10-phenanthroline to give osmapentalynes–silver(I)–phenanthroline adduct **4**. All the compounds have been characterized by X-ray diffraction analysis. The formation of these bimetallic adducts can be regarded as the “alkyne-like” interaction of an osmium–carbon triple bond with the coinage metal center. The interaction is weak and these adducts can readily dissociate to regenerate precursor osmapentalynes **1** in essentially quantitative yield with the assistance of PPh<sub>3</sub> or chloride ligands.



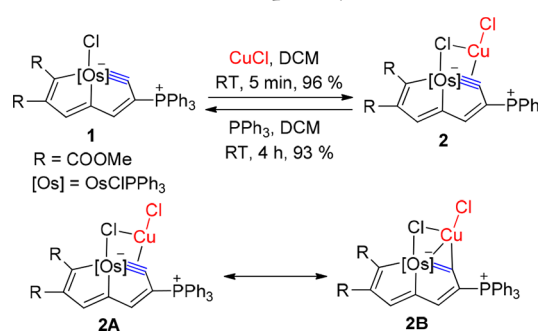
## INTRODUCTION

Metal carbonyne (or alkylidyne) complexes constitute an important class of organometallic complexes, which have attracted considerable attention because of their interesting reactivity<sup>1</sup> and application in catalysis.<sup>2</sup> The metal–carbon triple bond possesses “alkyne-like” character which can react with some metal complexes, generating the dimetalocyclopropene derivatives or polymetallic complexes with bridging carbonynes.<sup>3</sup> The formation of the M–M and M–C bonds in these reactions offer valuable information to understand the principles of catalytic reactions, especially for the multimetallic catalysis.<sup>4</sup> Various metal carbonyne complexes, e.g., chromium,<sup>5</sup> molybdenum,<sup>5,6</sup> tungsten,<sup>5–7</sup> manganese,<sup>8</sup> rhenium,<sup>8,9</sup> and osmium carbonynes,<sup>10</sup> with a second metal complex have been investigated in the literature. However, most of them are the acyclic metal carbonynes, the related chemistry of cyclic metal carbonyne complexes has scarcely been reported.<sup>11</sup>

Recently, we synthesized a type of five-membered cyclic osmium carbonyne complexes, i.e., osmapentalynes.<sup>12</sup> The carbonyne carbon bond angles in the osmapentalynes are around 130°, which are much smaller than those of the acyclic metal carbonynes. Such distortion makes a considerable large ring strain. Thus, the metal–carbon triple bond in osmapentalynes exhibits unique performances. For instance, it shows ambiphilic reactivity toward both nucleophiles<sup>13</sup> and electrophiles;<sup>14</sup> it performs cycloadditions with various alkynes.<sup>15</sup> The fascinating structural features and properties of the cyclic osmacarbonynes motivate us to explore their interactions with metal complexes. Herein, we report the reactions of an osmapentalynes with a complete set of coinage metal (Cu, Ag, and Au) complexes. A series of bimetallic adducts involving the interaction of the osmium–carbon triple bond with the coinage metal center have been obtained. Interestingly, the coinage metals can be efficiently relieved from the adducts to reproduce the osmapentalynes, reflecting the weak interaction between the two parts.

## RESULTS AND DISCUSSION

We initially investigated the reaction of osmapentalynes **1**<sup>15c</sup> with CuCl. As shown in Scheme 1, when the mixture of **1** and

Scheme 1. Reaction of Osmapentalynes **1** with CuCl

excess CuCl was stirred at room temperature for 5 min in dichloromethane, complex **2** was formed. It could be isolated as a yellow solid in 96% yield by flash column chromatography. Complex **2** was characterized by nuclear magnetic resonance (NMR) spectroscopy, and elemental analysis.

In the <sup>1</sup>H NMR, the signals of the two hydrogens from the metallacyclic skeleton in **2** were observed at 8.2 (C<sub>3</sub>H) and 8.8 (C<sub>5</sub>H) ppm, respectively, which were located in the typical region of metallaaromatics.<sup>16</sup> In the <sup>13</sup>C NMR spectrum, the characteristic low field signal at 293.6 ppm was attributed to C1 (Table 1), which was upshifted in comparison with that of complex **1** (325.8 ppm) but downshifted compared with those of previously reported osmapentalynes<sup>13a</sup> (210.0–250.5 ppm). It suggested that two major resonance forms **2A**

Received: April 11, 2018

Published: May 23, 2018

**Table 1.** Selected NMR Spectroscopic Data for the Complexes 1–4<sup>a</sup>

	$\delta$ ( <sup>13</sup> C) [ppm]		$\delta$ ( <sup>31</sup> P) [ppm]	
	C1		OsPPh <sub>3</sub>	CPPh <sub>3</sub>
1	325.8		−9.6	5.6
2	293.6		−15.2	7.5
3	304.6		−24.2	8.4
4	307.9		−22.5	8.3

<sup>a</sup>The NMR spectroscopic data of **1** selected from ref 15c.

(the osmacarbyne coordinated to the copper center) and **2B** (a dimetallacyclopropene unit) contributed to the structure of **2**, as shown in Scheme 1.

The structure of **2** was further confirmed by single-crystal X-ray diffraction. As shown in Figure 1, the osmium center

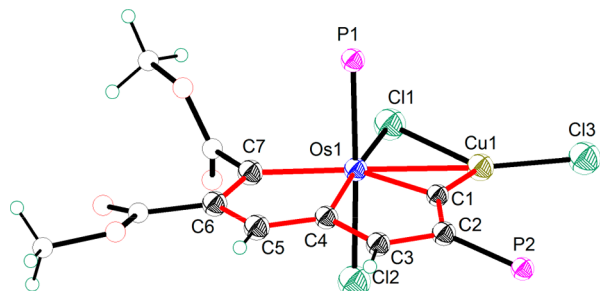


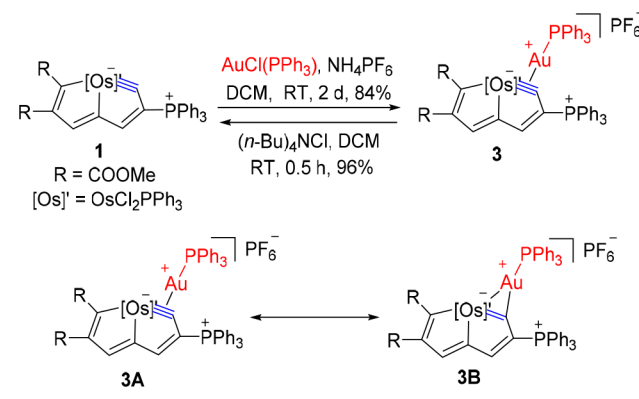
**Figure 1.** Molecular structure of **2** (50% probability thermal ellipsoids). The counteranion and phenyl moieties in PPh<sub>3</sub> were omitted for clarity.

adopts a distorted pentagonal bipyramidal geometry with the equatorial plane vertices occupied by three carbon atoms, one chlorine atom, and one copper atom. The fused metallatrimetallic moiety (Os1, C1–C7, and Cu1) of complex **2** is nearly coplanar, as reflected by the mean deviation from the least-squares plane of 0.0682 Å, indicating that the Cu atom almost sits in the same plane as the osmapentalyne unit. The carbonyne bond distance Os1–C1 (1.872(6) Å) increases by only 0.022 Å on coordination of CuCl (Table 2), indicating the  $\pi$ -back bonding is weak in complex **2**, and the resonance form **2A** is dominant. The Os–C triple bond coordinated to the Cu atom with the Os1–Cu1 and Cu1–C1 distances being 2.5400(9) and 1.913(6) Å, respectively. In particular, the Cu1–C1 distance

(1.913(6) Å) is within the range of typical Cu–C(aryl) bond lengths (1.849–2.020 Å),<sup>17</sup> indicating a dimetallacyclopropene form (**2B**) that can not be neglected. The Cu1 is also coordinated by two Cl atoms. The distance of Cu1–Cl3 (2.145(2) Å) is significantly shorter than that of Cu1–Cl1 (2.411(2) Å) where the Cl1 serves as  $\mu_2$  bridge between the Os and Cu atoms. Distances of C–C bonds (1.388(9)–1.404(9) Å) of the fused five-membered rings are between the C–C single- and double-bond lengths, suggesting the extensive electronic delocalization within the osmapentalyne ring in **2**. The reaction of acyclic metal carbonyne complexes with copper salts have been reported in the literature;<sup>5,10,18</sup> however, the related bimetallic copper salt adducts characterized by single-crystal X-ray diffraction are very limited. Complex **2** is the first structurally defined osmacarbyne-copper salt adduct.

Interestingly, when **2** was treated with PPh<sub>3</sub> in dichloromethane at room temperature for 4 h, osmapentalyne **1** could be regenerated in 93% yield. The facile and efficient conversion reflects the weak interaction between CuCl and the osmacarbyne. Cleavages of the metal salts from the tungsten or molybdenum carbonyne-metal salt adducts have been observed when they were treated with donor ligands,<sup>6,19</sup> such as tetrahydrofuran,<sup>6c</sup> carbon monoxide,<sup>6a</sup> PMe<sub>3</sub>,<sup>19a</sup> or sulfur.<sup>19b</sup>

As shown in Scheme 2, complex **1** can also react with AuCl(PPh<sub>3</sub>). When the mixture of complex **1**, AuCl(PPh<sub>3</sub>), and

**Scheme 2.** Reaction of Osmapentalyne **1** with AuCl(PPh<sub>3</sub>)

NH<sub>4</sub>PF<sub>6</sub> was stirred at room temperature for 2 d, complex **3** could be afforded as a yellow solid in 84% yield. The <sup>31</sup>P{<sup>1</sup>H}

**Table 2.** Selected Bond Lengths and Angles for 1–4<sup>a</sup>

	1	2 M = Cu	3 M = Au	4 M = Ag		1	2 M = Cu	3 M = Au	4 M = Ag
bond lengths [Å]					bond angles [deg]				
Os1–C1	1.850(6)	1.872(6)	1.875(7)	1.854(4)	Os1–C1–C2	127.9(5)	127.7(5)	131.6(6)	129.7(3)
C1–C2	1.426(9)	1.392(8)	1.366(11)	1.406(6)	C1–C2–C3	108.3(5)	108.5(6)	107.5(7)	108.0(4)
C2–C3	1.400(9)	1.404(9)	1.411(11)	1.396(6)	C2–C3–C4	111.7(6)	112.4(6)	110.3(8)	111.4(4)
C3–C4	1.410(9)	1.400(9)	1.389(11)	1.403(6)	C3–C4–Os1	117.8(5)	117.3(5)	119.8(6)	118.4(3)
Os1–C4	2.079(6)	2.076(6)	2.098(8)	2.092(4)	C4–Os1–C1	73.9(3)	73.9(3)	70.6(3)	72.51(18)
C4–C5	1.373(9)	1.388(10)	1.384(11)	1.386(6)	Os1–C4–C5	119.2(5)	118.6(5)	117.4(6)	118.7(3)
C5–C6	1.411(9)	1.393(9)	1.397(12)	1.416(6)	C4–C5–C6	113.4(6)	113.3(6)	114.2(8)	112.9(4)
C6–C7	1.381(9)	1.388(9)	1.373(12)	1.378(6)	C5–C6–C7	112.6(6)	114.1(6)	113.3(8)	112.8(4)
C7–Os1	2.045(6)	2.049(7)	2.045(9)	2.032(4)	C6–C7–Os1	120.6(5)	119.0(5)	120.3(6)	121.3(3)
M1–Os1		2.5400(9)	2.8549(4)	2.8722(4)	C7–Os1–C4	74.1(2)	74.9(3)	74.6(3)	74.25(17)
M1–C1		1.913(6)	2.072(7)	2.144(4)	Os1–M1–C1		47.18(19)	41.00(19)	40.18(12)
					C1–Os1–M1		48.54(18)	46.5(2)	48.25(12)
					M1–C1–Os1		84.3(2)	92.5(3)	91.56(18)

<sup>a</sup>The bond lengths and angles of **1** selected from ref 15c.

NMR spectrum showed the AuPPh<sub>3</sub> signal at 45.8 ppm, the signals of CPh<sub>3</sub> at 8.4 ppm and the signal of OsPPh<sub>3</sub> at −24.2 ppm. In the <sup>13</sup>C NMR spectrum, the resonance of C1 (304.6 ppm) was upshifted in comparison with that of **1** (325.8 ppm, Table 1) but downshifted than the reported osmapentalenes<sup>13a</sup> (210.0–250.5 ppm), indicating the contribution of resonance forms **3A** and **3B**.

The structure of **3** was further confirmed by X-ray diffraction (Figure 2). The eight atoms of the osmapentalene ring

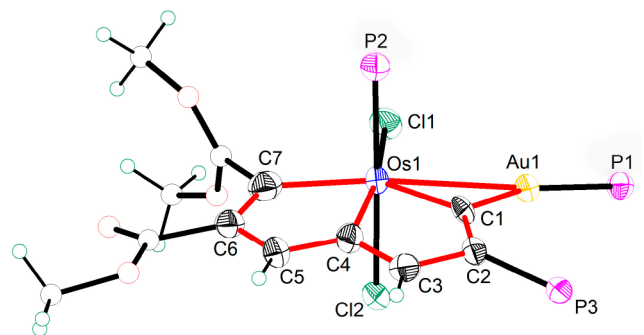


**Figure 2.** Molecular structure of **3** (50% probability thermal ellipsoids). The counteranion and phenyl moieties in PPh<sub>3</sub> were omitted for clarity.

(Os1, C1–C7) remain coplanar with the mean deviation from the least-squares plane of 0.0291 Å. The Au atom locates out of the osmapentalene plane slightly, with the dihedral angle of the dimetallacyclopentene plane and the osmapentalene plane of 16.8°. The Os1–C1 bond length of **3** is slightly stretched (0.025 Å) in comparison with that of **1** (Table 2), suggesting the osmium carbene character retains and the resonance structure **3A** is dominant. The Os1–Au1 distance is 2.8549(4) Å. The Au1–C1 bond length (2.072(7) Å) locates in the range of typical Au–C(aryl) bond lengths (1.871–2.225 Å),<sup>17</sup> indicating the contribution of resonance structure **3B**. Due to the steric effect of PPh<sub>3</sub> ligand on the Au center, the bond angle of Au1–Os1–Cl1 (72.85(5)°) is much larger than the Cu1–Os1–Cl1 angle of complex **2** (57.64(5)°). Consistently, the Au1 and Cl1 distance is 3.146 Å, which is far away to be considered as a bond. This is different from copper adduct **2** in which the Cl1 bridged the Os1 and Cu1 atoms with the Cu1–Cl1 being 2.411(2) Å. The interaction between Au and osmapentalene unit is weak and can be easily eliminated by Cl ligand. Osmapentalene **1** could be regenerated in 96% yield within half an hour when **3** was treated with (*n*-Bu)<sub>4</sub>NCl (Scheme 2).

The  $\pi$ -bonding of cationic gold moiety, such as cationic gold phosphine ([Au(PR<sub>3</sub>)<sup>+</sup>], with various unsaturated ligands, including alkene, alkyne, diene, allene, and enol ether, have been reported in the literature.<sup>20</sup> These species aroused a wide interest owing to the potential relevance to the intermediates in the gold-catalyzed functionalization of C–C multiple bonds.<sup>21</sup> However, cationic gold phosphine ([Au(PR<sub>3</sub>)<sup>+</sup>] moiety binding with the “alkyne-like” metal carbene unit is relatively limited.<sup>22</sup> A structurally defined example related to complex **3** is the [Au(PPh<sub>3</sub>)<sup>+</sup>–tungsten–carbene adduct reported by Stone and coauthors.<sup>22a</sup> By comparison, the length of the metal–carbon bond in the case of tungsten–carbene increases by 0.06 Å through the coordination to the Au center,<sup>22a</sup> which is longer than that in complex **3** (0.025 Å).

We further investigated the reactions of **1** and silver salt. When **1** was treated with AgOTf, a main product with the

signals observed at 6.9 and −17.5 ppm can be identified by *in situ* <sup>31</sup>P NMR. Attempts of isolation were failed due to its high instability. Fortunately, when the reaction of osmapentalene **1** with AgOTf were carried in the presence of 1,10-phenanthroline, a stable osmapentalene–silver(I)–phenanthroline adduct **4** could be isolated in a yield of 81%. Complex **4** was characterized by NMR spectroscopy and elemental analysis. The <sup>31</sup>P NMR showed the chemical shifts of CPh<sub>3</sub> and OsPPh<sub>3</sub> at 8.3 and −22.5 ppm, respectively. In <sup>13</sup>C NMR, the signal of carbene carbon atom was observed at 307.9 ppm, which was upshifted in comparison with that of complex **1** (325.8 ppm, Table 1) but downshifted compared with those of osmapentalenes<sup>13a</sup> (210.0–250.5 ppm). The structure of **4** could be also presented by the two major resonance forms, **4A** and **4B**.

The X-ray single-crystal diffraction experiment has been carried out to clarify the structure of **4**. As shown in Figure 3,

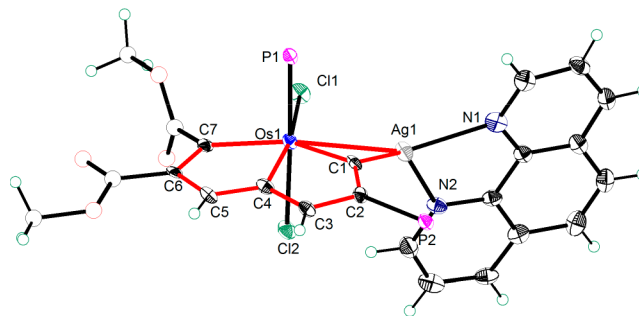


**Figure 3.** Molecular structure of **4** (50% probability thermal ellipsoids). The counteranion and phenyl moieties in PPh<sub>3</sub> were omitted for clarity.

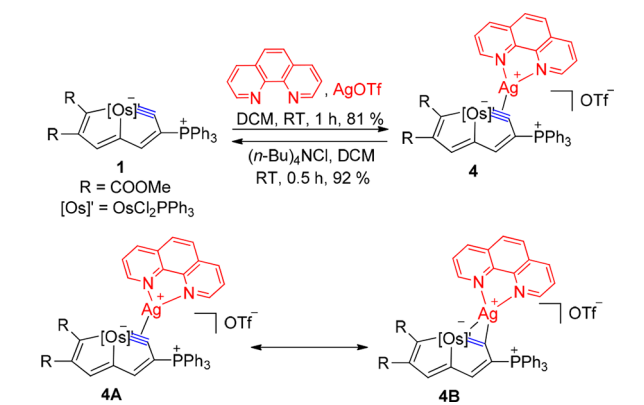
the overall structure of complex **4** is similar to that of **3**. The osmium center of **4** adopts a distorted pentagonal bipyramidal geometry. The metallacycle is basically coplanar, as reflected by the small mean deviation from the least-squares plane of 0.0226 Å. The Ag atom is located slightly out of the osmapentalene plane, with the dihedral angle of the dimetallacyclopentene plane and the osmapentalene plane of 20.8°. The Ag atom is further chelated by a phenanthroline ligand which is tend to vertically located toward the osmapentalene unit. The dihedral angle of the osmapentalene plane and the phenanthroline is 86.1°.

The Os1–C1 bond length of **4** (1.854(4) Å) was almost identical to that of **1** (1.850(6) Å), suggesting the weak interaction between the Ag fragment and the osmacarbene unit (Table 2). Roper and co-authors reported the reaction of an acyclic osmacarbene Os(≡CR)Cl(CO)(PPh<sub>3</sub>)<sub>2</sub> (R = *p*-tolyl) with AgCl.<sup>10</sup> The Os–C bond length increased by 0.07 Å on coordination of AgCl, which is more significant than that in complex **4**. The Os1–Ag1 bond length of **4** is 2.8722(4) Å, which is longer than that of the acyclic osmacarbene–AgCl adduct (2.799(1) Å). The Ag1–C1 distances of **4** (2.144(4) Å) is within the range of typical Ag–C(aryl) bond lengths (1.897–2.167 Å),<sup>17</sup> indicating the contribution of resonance structure **4B**.

Osmapentalene **1** could be easily regenerated from complex **4** by the cleavage of the cationic silver moiety in the presence of (*n*-Bu)<sub>4</sub>NCl (Scheme 3). By contrast, the acyclic osmacarbene–AgCl adduct could dissociate the AgCl moiety in the presence of HClO<sub>4</sub>, however, leading to an osmacarbene complex through the simultaneous protonation of the carbene unit.<sup>10</sup>

As a distinct class of aromatics, metallaromatics can undergo characteristic reactions of aromatics.<sup>16</sup> For example,

**Scheme 3.** Reaction of Osmapentalyne **1** with AgOTf and 1,10-Phenanthroline



metallabenzenes can react with other metal complexes as  $\eta^6$  ligands.<sup>23</sup> Our previous work showed the aromaticity of these cyclic osmacarbyne complex species.<sup>12a</sup> In this case, complex **1** coordinated to coinage metal salts via the osmacarbyne unit rather than the aromatic rings. We inferred that the large ring strains associated with extreme distortion of the osmacarbyne unit results in the highly reactivity of Os–C triple bonds, as exemplified by the abundant reactions of cyclic osmacarbyne complex species.<sup>13–15</sup>

To better understand the interaction between coinage metal salts and osmacarbyne unit, we performed density functional theory (DFT) calculations<sup>24</sup> on complexes **1–4**. The Wiberg bond indices (WBI)<sup>25</sup> of the bonds around the osmium center and coinage metal centers are provided in Figure 4. The WBI of

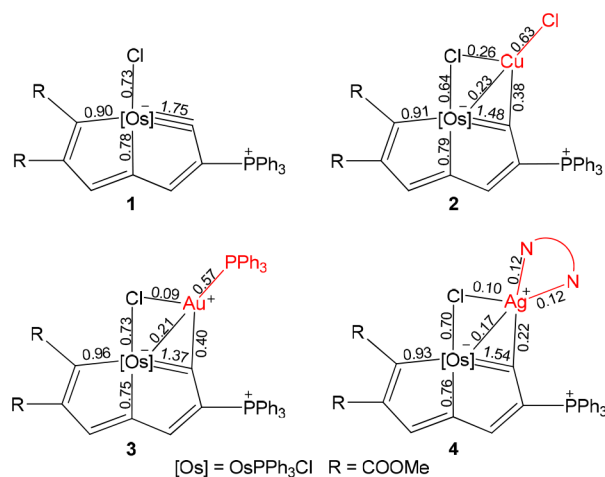


**Figure 4.** Wiberg bond indices of the bonds around the osmium center and coinage metal centers.

Os–C carbyne bonds in complexes **2** (1.48), **3** (1.37), and **4** (1.54) are smaller than that of complex **1** (1.75), which may be attribute to the coordination with the coinage metal salts. The calculated WBI of the coinage metals with osmacarbyne units are 0.38 (Cu–C), 0.23 (Os–Cu), 0.40 (Au–C), 0.21 (Os–Au), 0.22 (Ag–C), and 0.17 (Os–Ag), which are consistent with the expected trend in resonance forms **2A**, **3A**, and **4A**. In addition, the WBI calculated for the  $\mu_2$ -Cl bridge in **2** are 0.64 (Os–Cl1) and 0.26 (Cu–Cl1). Nevertheless, the interactions of Au–Cl1 (0.09) in **3** and Ag–Cl1 (0.10) in **4** are negligible. These data are in good agreement with the experimental observed bond distances.

The solid-state thermal stabilities of these bimetallic complexes have been performed in air by heating for 3 h. As shown in Table 3, copper and gold adducts **2** and **3** exhibit

**Table 3.** Thermal Decomposition Data of Complexes **1–4** in the Solid State<sup>a</sup>

	100 °C	125 °C	150 °C	200 °C
<b>1</b>	●	●	▲	■
<b>2</b>	●	●	●	●
<b>3</b>	●	●	●	■
<b>4</b>	●	▲	■	

<sup>a</sup>All reactions were performed for 3 h in air. ● = stable; ▲ = partly decomposed; ■ = completely decomposed.

higher thermal stabilities than the parent osmapentalyne **1**. Silver adduct **4** is more liable to decompose than **1**. This is probably due to the silver complex is well-known for its susceptibility to oxidation. It is interesting that although the interaction between CuCl or [Au(PPh<sub>3</sub>)]<sup>+</sup> and osmapentalyne are weak, the thermal stabilities of the corresponding Cu/Au adducts are significantly enhanced. The metal salt moieties provide effective protection to the osmapentalyne, which suppress the activity of the osmium carbyne unit. In addition, the metals can be efficiently relieved from the adducts to reproduce osmacarbyne **1**. In this regards, the facilely interconversion process can be viewed as the protection–deprotection reactions of osmacarbyne unit, which is promising for its future application.

## CONCLUSION

In summary, reactions of a cyclic osmacarbyne with the complete set of coinage metal complexes have been investigated. A series of novel bimetallic complexes with osmapentalyne unit are obtained. The cyclic osmacarbyne–coinage metal adducts can be represented by two major resonance structures, a  $\pi$ -coordinated form and a dimetalocyclopropene form, with the former providing more contribution. The interaction between cyclic osmacarbyne with coinage metal is weak, which can be readily dissociated to regenerate the original cyclic osmacarbyne in the presence of ligands. This work demonstrates the first systematic investigation of cyclic metal carbyne complexes with coinage metal complexes. It may promote new understanding of the chemistry of metal carbyne complexes, encouraging further efforts to realize their applications such as in catalytic transformations.

## EXPERIMENTAL SECTION

**General Methods.** All syntheses were performed under an inert atmosphere (N<sub>2</sub>) using standard Schlenk techniques, unless otherwise stated. Reagents were used as received from commercial sources without further purification. Starting material **1** was synthesized according to a previously published procedure.<sup>15c</sup> Nuclear magnetic resonance (NMR) spectroscopic experiments were performed on a Bruker Advance III 400 spectrometer (<sup>1</sup>H, 400.1 MHz; <sup>13</sup>C, 100.6 MHz; <sup>31</sup>P, 162.0 MHz) or a Bruker Advance III 500 spectrometer (<sup>1</sup>H, 500.2 MHz; <sup>13</sup>C, 125.8 MHz; <sup>31</sup>P, 202.5 MHz) or a Bruker Ascend III 600 spectrometer (<sup>1</sup>H, 600.1 MHz; <sup>13</sup>C, 150.9 MHz; <sup>31</sup>P, 242.9 MHz) at room temperature. The <sup>1</sup>H and <sup>13</sup>C NMR chemical shifts ( $\delta$ ) are relative to tetramethylsilane, and the <sup>31</sup>P NMR chemical shifts are relative to 85% H<sub>3</sub>PO<sub>4</sub>. The absolute values of the coupling constants are given in hertz (Hz). Multiplicities are abbreviated as singlet (s), doublet (d), triplet (t), multiplet (m), quartet (q), quintet (quint) and broad (br). Elemental analysis data were obtained on an Elementar Analysensysteme GmbH Vario EL III instrument.

Table 4. Crystal Data and Structure Refinement for 2–4

	2·3C <sub>2</sub> H <sub>4</sub> Cl <sub>2</sub>	3·2.5SCH <sub>2</sub> Cl <sub>2</sub> ·0.75SCH <sub>3</sub> OH·0.5H <sub>2</sub> O	4·2CH <sub>2</sub> Cl <sub>2</sub>
formula	C <sub>53</sub> H <sub>50</sub> Cl <sub>9</sub> CuO <sub>4</sub> OsP <sub>2</sub>	C <sub>68.25</sub> H <sub>60.25</sub> AuCl <sub>7</sub> F <sub>6</sub> O <sub>3.25</sub> OsP <sub>4</sub>	C <sub>62</sub> H <sub>50</sub> AgCl <sub>6</sub> F <sub>3</sub> N <sub>2</sub> O <sub>7</sub> OsP <sub>2</sub> S
M <sub>r</sub>	1385.66	1837.61	1596.81
crystal system	monoclinic	triclinic	triclinic
space group	P2 <sub>1</sub> /c	P $\bar{1}$	P $\bar{1}$
a [Å]	19.5821(5)	11.4732(3)	13.4597(5)
b [Å]	14.3644(4)	13.4682(5)	14.1277(6)
c [Å]	19.8903(5)	23.8946(7)	19.0956(8)
α [°]	90	86.5360(10)	103.457(4)
β [°]	92.899(2)	88.5210(10)	97.299(3)
γ [°]	90	89.7440(10)	116.967(4)
V [Å <sup>3</sup> ]	5587.7(3)	3684.3(2)	3032.0(2)
Z	4	2	2
ρ <sub>calcd</sub> [g cm <sup>-3</sup> ]	1.647	1.656	1.749
μ [mm <sup>-1</sup> ]	3.184	4.114	2.833
F (000)	2752.0	1800.0	1580.0
2θ range [°]	5.484–49.998	6.062–49.998	6.638–53.996
reflns collected	28473	28546	25028
independent reflns	9825	12877	12216
observed reflns [I ≥ 2σ(I)]	7946	10306	10250
data/restraints/params	9825/24/631	12877/30/868	12216/0/768
GOF on F <sup>2</sup>	1.046	1.097	1.054
R <sub>1</sub> /wR <sub>2</sub> [I ≥ 2σ(I)]	0.0504/0.1159	0.0485/0.1203	0.0432/0.0966
R <sub>1</sub> /wR <sub>2</sub> (all data)	0.0688/0.1260	0.0647/0.1423	0.0577/0.1063
largest peak/hole [e Å <sup>-3</sup> ]	1.41/−1.41	2.04/−1.75	2.15/−2.57
CCDC nos. <sup>a</sup>	1834299	1834301	1834303

<sup>a</sup>These files contain the supplementary crystallographic data for this paper. These data can be obtained free of charge from The Cambridge Crystallographic Data Centre via [www.ccdc.cam.ac.uk/data\\_request/cif](http://www.ccdc.cam.ac.uk/data_request/cif).

**Preparation of Complex 2.** A mixture of **1** (200 mg, 0.20 mmol) and cuprous chloride (198 mg, 2.00 mmol) in dichloromethane (10 mL) was stirred at room temperature for 5 min to give a brown solution. The excess cuprous chloride was removed by filtration. The filtrate was concentrated to ca. 2 mL, the residue was purified by column chromatography (silica gel, 200–300 mesh, eluent: dichloromethane/acetone = 10:1) to afford **2** as a yellow solid. Yield: 209 mg, 96%. <sup>1</sup>H NMR (400.1 MHz, CD<sub>2</sub>Cl<sub>2</sub>): δ = 8.8 (s, 1H, C<sup>5</sup>H), 8.2 (s, 1H, C<sup>3</sup>H), 7.7–7.1 (30H, other aromatic protons), 3.7 and 3.6 ppm (s, 6H, C<sup>9</sup>H and C<sup>11</sup>H). <sup>31</sup>P NMR (162.0 MHz, CD<sub>2</sub>Cl<sub>2</sub>): δ = 7.5 (s, C<sup>1</sup>PPh<sub>3</sub>), −15.2 ppm (s, OsPPh<sub>3</sub>). <sup>13</sup>C NMR (100.6 MHz, CD<sub>2</sub>Cl<sub>2</sub>, plus <sup>13</sup>C DEPT-135, <sup>1</sup>H–<sup>13</sup>C HSQC and <sup>1</sup>H–<sup>13</sup>C HMBC): δ = 293.6 (br, C1), 220.1 (br, C7), 187.5 (d, J = 23.3 Hz, C4), 176.1 and 162.9 (s, C8 and C10, confirmed by <sup>1</sup>H–<sup>13</sup>C HMBC), 159.7 (d, J = 16.0 Hz, C3), 154.9 (s, C6), 151.2 (s, C5), 134.8 (d, J = 81.2 Hz, C2, confirmed by <sup>1</sup>H–<sup>13</sup>C HMBC), 134.4–117.8 (other aromatic carbons), 51.2 and 50.8 ppm (s, C9 and C11). Elemental analysis calcd (%) for C<sub>47</sub>H<sub>38</sub>Cl<sub>3</sub>CuO<sub>4</sub>OsP<sub>2</sub>: C 51.84, H 3.52; found: C 51.72, H 3.67.

**Preparation of Complex 3.** A mixture of **1** (200 mg, 0.20 mmol), AuCl(PPh<sub>3</sub>) (495 mg, 1.00 mmol), and ammonium hexafluorophosphate (326 mg, 2.00 mmol) in dichloromethane (10 mL) was stirred at room temperature for 2 days to give a brown solution. The excess ammonium hexafluorophosphate was removed by filtration, and the filtrate was evaporated under vacuum to approximately 2 mL. The residue was purified by column chromatography (silica gel, 200–300 mesh, eluent: dichloromethane/acetone = 10:1) to afford **3** as a yellow solid. Yield: 268 mg, 84%. <sup>1</sup>H NMR (500.2 MHz, CD<sub>2</sub>Cl<sub>2</sub>): δ = 8.8 (s, 1H, C<sup>5</sup>H), 7.9 (s, 1H, C<sup>3</sup>H), 7.7–7.0 (45H, other aromatic protons) 3.7 and 3.6 ppm (s, 6H, C<sup>9</sup>H and C<sup>11</sup>H). <sup>31</sup>P NMR (202.5 MHz, CD<sub>2</sub>Cl<sub>2</sub>): δ = 45.8 (s, AuPPh<sub>3</sub>), 8.4 (s, C<sup>1</sup>PPh<sub>3</sub>), −24.2 (s, OsPPh<sub>3</sub>), −144.4 ppm (quint, J = 710.9 Hz, PF<sub>6</sub>). <sup>13</sup>C NMR (125.8 MHz, CD<sub>2</sub>Cl<sub>2</sub>, plus <sup>13</sup>C DEPT-135, <sup>1</sup>H–<sup>13</sup>C HSQC and <sup>1</sup>H–<sup>13</sup>C HMBC): δ = 304.6 (ddd, J = 63.9 Hz, J = 20.6 Hz, J = 11.1 Hz, C1), 220.2 (br, C7), 184.5 (dd, J = 22.9 Hz, J = 3.8 Hz, C4), 175.8 and 161.6 (s, C8 and C10, confirmed by <sup>1</sup>H–<sup>13</sup>C HMBC), 160.3 (d, J = 16.8 Hz, C3), 154.2 (s, C5), 153.3 (s, C6), 137.4 (d, J = 94.1 Hz, C2, confirmed by <sup>1</sup>H–<sup>13</sup>C HMBC), 135.2–117.0

(other aromatic carbons), 51.7 and 51.3 ppm (s, C9 and C11). Elemental analysis calcd (%) for C<sub>65</sub>H<sub>53</sub>AuCl<sub>2</sub>F<sub>6</sub>O<sub>4</sub>OsP<sub>4</sub>: C 48.97, H 3.35; found: C 49.32, H 3.02.

**Preparation of Complex 4.** A mixture of **1** (200 mg, 0.20 mmol), AgOTf (102 mg, 0.40 mmol), and 1,10-phenanthroline monohydrate (360 mg, 2.0 mmol) in dichloromethane (10 mL) was stirred at room temperature for 1 h to give a brown solution. The excess AgOTf was removed by filtration, and the filtrate was evaporated under vacuum to approximately 2 mL. The residue was purified by column chromatography (silica gel, 200–300 mesh, eluent: dichloromethane/acetone = 5:1) to afford **4** as a yellow solid. Yield: 231 mg, 81%. <sup>1</sup>H NMR (600.1 MHz, CD<sub>2</sub>Cl<sub>2</sub>): δ = 8.9 (s, 1H, C<sup>5</sup>H), 8.8 (d, J = 4.1 Hz, 2H, protons of 1,10-phenanthroline), 8.4 (d, J = 7.5 Hz, 2H, protons of 1,10-phenanthroline), 8.0 (s, 1H, C<sup>3</sup>H), 7.9–7.2 (34H, other aromatic protons), 3.7 and 3.6 ppm (s, 6H, C<sup>9</sup>H and C<sup>11</sup>H). <sup>31</sup>P NMR (242.9 MHz, CD<sub>2</sub>Cl<sub>2</sub>): δ = 8.3 (s, C<sup>1</sup>PPh<sub>3</sub>), −22.5 ppm (s, OsPPh<sub>3</sub>). <sup>13</sup>C NMR (150.9 MHz, CD<sub>2</sub>Cl<sub>2</sub>, plus <sup>13</sup>C DEPT-135, <sup>1</sup>H–<sup>13</sup>C HSQC and <sup>1</sup>H–<sup>13</sup>C HMBC): δ = 307.9 (br, C1), 221.8 (d, J = 9.0 Hz, C7), 183.9 (d, J = 22.1 Hz, C4), 175.8 and 162.2 (s, C8 and C10), 159.6 (d, J = 16.3 Hz C3), 154.0 (s, C5), 152.6 (s, C6), 150.8.0–134.4 (other aromatic carbons), 134.1 (d, J = 94.6 Hz, C2), 133.5–117.0 (other aromatic carbons and the carbon atom of OTf− (s, 119.3)), 51.4 and 50.4 ppm (s, C9 and C11). Elemental analysis calcd (%) for C<sub>60</sub>H<sub>46</sub>AgCl<sub>2</sub>F<sub>3</sub>N<sub>2</sub>O<sub>7</sub>OsP<sub>2</sub>S: C 50.50, H 3.25, N 1.96; found: C 50.15, H 3.62, N 2.20.

**Regeneration of 1 from 2–4.** (a) A mixture of **2** (100 mg, 0.09 mmol) and triphenylphosphine (118 mg, 0.45 mmol) in dichloromethane (10 mL) was stirred at room temperature for 4 h to give a brown solution. The solid was removed by filtration and the filtrate was evaporated under vacuum to approximately 2 mL. The residue was purified by column chromatography (silica gel, 200–300 mesh, eluent: dichloromethane/acetone = 5:1) to afford **1** as a yellow solid. Yield: 83 mg, 93%. (b) A mixture of **3** (100 mg, 0.06 mmol) and tetra-*n*-butylammonium chloride (25 mg, 0.09 mmol) in dichloromethane (10 mL) was stirred at room temperature for 0.5 h to give a brown solution. The solvent was evaporated under vacuum to approximately 2 mL. The residue was purified by column chromatography (silica gel,

200–300 mesh, eluent: dichloromethane/acetone = 5:1) to afford **1** as a yellow solid. Yield: 57 mg, 96%. (c) A mixture of **4** (100 mg, 0.07 mmol) and tetra-*n*-butylammonium chloride (30 mg, 0.11 mmol) in dichloromethane (10 mL) was stirred at room temperature for 0.5 h to give a brown solution. The solid was removed by filtration, and the filtrate was evaporated under vacuum to approximately 2 mL and washed with Et<sub>2</sub>O (3 × 20 mL) to afford a yellow solid. The solid of the mixture was purified by column chromatography (silica gel, 200–300 mesh, eluent: dichloromethane/acetone = 5:1) to give complex **1** as a yellow solid. Yield: 64 mg, 92%.

**Crystallographic Analysis.** A crystal of **2** suitable for X-ray diffraction was grown from a 1,2-dichloroethane solution layered with hexane. A crystal suitable for X-ray diffraction of **3** was grown from a dichloromethane/methanol solution layered with hexane. A crystal of **4** suitable for X-ray diffraction was grown from a dichloromethane solution layered with hexane. Single-crystal X-ray diffraction data were collected on an Oxford Gemini S Ultra CCD Area Detector (**2**), a Rigaku R-Axis SPIDER IP CCD area detector (**3**) or an Agilent SuperNova diffractometer (**4**) with graphite-monochromated Mo K $\alpha$  radiation ( $\lambda = 0.71073$  Å). All the data were corrected for absorption effects using a multiscan technique. All the structures were solved by the Patterson function, completed by subsequent difference Fourier map calculations, and refined by a full-matrix least-squares method on  $F^2$  using the SHELXTL program package. All non-hydrogen atoms were refined anisotropically unless otherwise stated. The hydrogen atoms were placed at their idealized positions and assumed the riding model unless otherwise stated. The methanol (CH<sub>3</sub>OH) solvent and H<sub>2</sub>O molecule in **3** was refined without the addition of H atoms. X-ray crystal structure information is available at the Cambridge Crystallographic Data Centre (CCDC) under deposition numbers CCDC 1834299 (**2**), CCDC 1834301 (**3**), and CCDC 1834303 (**4**). For details on the crystal data, data collection, and refinements, see Table 4.

**Density Functional Theory (DFT) Calculations.** All structures were optimized at the B3LYP level of DFT.<sup>24</sup> Additionally, frequency calculations were also performed to identify all the stationary points as minima (zero imaginary frequency). In the B3LYP calculations, the effective core potentials (ECPs) of Hay and Wadt with a double- $\zeta$  valence basis set (LanL2DZ)<sup>26</sup> were used to describe the Os, Cu, Ag, Au, Cl, and P atoms, whereas the standard 6-31G basis set was used for the C, O, N, and H atoms. Polarization functions were added for Os ( $\zeta(f) = 0.886$ ), Cu ( $\zeta(f) = 3.525$ ), Ag ( $\zeta(f) = 1.611$ ), Au ( $\zeta(f) = 1.050$ ), Cl ( $\zeta(d) = 0.514$ ), and P ( $\zeta(d) = 0.340$ )<sup>27</sup> in all calculations. All the optimizations were performed with the Gaussian 09 software package.<sup>28</sup> Wiberg bond index<sup>25</sup> calculations were carried out with the NBO 6.0 program<sup>29</sup> interfaced with the Gaussian 09 program.

## ■ ASSOCIATED CONTENT

### Supporting Information

The Supporting Information is available free of charge on the ACS Publications website at DOI: 10.1021/acs.organomet.8b00214.

Crystallographic data for complexes **2–4** and copies of <sup>1</sup>H, <sup>31</sup>P, and <sup>13</sup>C NMR spectra of all new products (PDF) Cartesian coordinates of the calculated structures **1–4** (XYZ)

### Accession Codes

CCDC 1834299, 1834301, and 1834303 contain the supplementary crystallographic data for this paper. These data can be obtained free of charge via [www.ccdc.cam.ac.uk/data\\_request/cif](http://www.ccdc.cam.ac.uk/data_request/cif), or by emailing [data\\_request@ccdc.cam.ac.uk](mailto:data_request@ccdc.cam.ac.uk), or by contacting The Cambridge Crystallographic Data Centre, 12 Union Road, Cambridge CB2 1EZ, UK; fax: +44 1223 336033.

## ■ AUTHOR INFORMATION

### Corresponding Authors

\*E-mail: [linyum@xmu.edu.cn](mailto:linyum@xmu.edu.cn).

\*E-mail: [hpxia@xmu.edu.cn](mailto:hpxia@xmu.edu.cn).

### ORCID

Xiaoxi Zhou: 0000-0002-8107-2000

Hong Zhang: 0000-0003-3010-0806

Yu-Mei Lin: 0000-0002-7287-9873

Haiping Xia: 0000-0002-2688-6634

### Notes

The authors declare no competing financial interest.

## ■ ACKNOWLEDGMENTS

We gratefully acknowledge the NSFC (Nos. 21332002, 21490573, and 21671164) for their financial support.

## ■ REFERENCES

- (a) Jia, G. *Coord. Chem. Rev.* **2007**, *251*, 2167–2187. (b) Bolaño, T.; Esteruelas, M. A.; Oñate, E. *J. Organomet. Chem.* **2011**, *696*, 3911–3923. (c) Shi, C.; Jia, G. *Coord. Chem. Rev.* **2013**, *257*, 666–701.
- (a) Schrock, R. R. *Chem. Commun.* **2013**, *49*, 5529–5531. (b) Fürstner, A. *Angew. Chem., Int. Ed.* **2013**, *52*, 2794–2819.
- Stone, F. G. A. *Angew. Chem., Int. Ed. Engl.* **1984**, *23*, 89–99.
- (a) Buchwalter, P.; Rosé, J.; Braunstein, P. *Chem. Rev.* **2015**, *115*, 28–126. (b) Yuan, J.; Sun, T.; He, X.; An, K.; Zhu, J.; Zhao, L. *Nat. Commun.* **2016**, *7*, 11489.
- Dossett, S. J.; Hill, A. F.; Howard, J. A. K.; Nasir, B. A.; Spaniol, T. P.; Sherwood, P.; Stone, F. G. A. *J. Chem. Soc., Dalton Trans.* **1989**, 1871–1878.
- (a) Carriedo, G. A.; Howard, J. A. K.; Marsden, K.; Stone, F. G. A.; Woodward, P. *J. Chem. Soc., Dalton Trans.* **1984**, 1589–1595. (b) Jeffery, J. C.; Jelliss, P. A.; Stone, F. G. A. *Organometallics* **1994**, *13*, 2651–2661. (c) Ellis, D. D.; Farmer, J. M.; Malget, J. M.; Mullica, D. F.; Stone, F. G. A. *Organometallics* **1998**, *17*, 5540–5548.
- Colebatch, A. L.; Hill, A. F. *Dalton Trans.* **2017**, *46*, 4355–4365.
- Zhang, L.; Xiao, N.; Xu, Q.; Sun, J.; Chen, J. *Organometallics* **2005**, *24*, 5807–5816.
- Zhu, B.; Yu, Y.; Chen, J.; Wu, Q.; Liu, Q. *Organometallics* **1995**, *14*, 3963–3969.
- Clark, G. R.; Cochrane, C. M.; Roper, W. R.; Wright, L. J. *J. Organomet. Chem.* **1980**, *199*, C35–C38.
- Zhuo, Q.; Zhang, H.; Hua, Y.; Kang, H.; Zhou, X.; Lin, X.; Chen, Z.; Lin, J.; Zhuo, K.; Xia, H. *Sci. Adv.* **2018**, accepted, DOI: 10.1126/sciadv.aat0336.
- (a) Zhu, C.; Li, S.; Luo, M.; Zhou, X.; Niu, Y.; Lin, M.; Zhu, J.; Cao, Z.; Lu, X.; Wen, T. B.; Xie, Z.; Schleyer, P. v. R.; Xia, H. *Nat. Chem.* **2013**, *5*, 698–703. (b) Zhu, C.; Yang, Y.; Wu, J.; Luo, M.; Fan, J.; Zhu, J.; Xia, H. *Angew. Chem., Int. Ed.* **2015**, *54*, 7189–7192. (c) Zhuo, Q.; Lin, J.; Hua, Y.; Zhou, X.; Shao, Y.; Chen, S.; Chen, Z.; Zhu, J.; Zhang, H.; Xia, H. *Nat. Commun.* **2017**, *8*, 1912.
- (a) Zhu, C.; Luo, M.; Zhu, Q.; Zhu, J.; Schleyer, P. v. R.; Wu, J. I. C.; Lu, X.; Xia, H. *Nat. Commun.* **2014**, *5*, 3265. (b) Zhu, C.; Zhu, Q.; Fan, J.; Zhu, J.; He, X.; Cao, X. Y.; Xia, H. *Angew. Chem., Int. Ed.* **2014**, *53*, 6232–6236. (c) Zhu, Q.; Zhu, C.; Deng, Z.; He, G.; Chen, J.; Zhu, J.; Xia, H. *Chin. J. Chem.* **2017**, *35*, 628–634. (d) Luo, M.; Long, L.; Zhang, H.; Yang, Y.; Hua, Y.; Liu, G.; Lin, Z.; Xia, H. *J. Am. Chem. Soc.* **2017**, *139*, 1822–1825.
- (a) Luo, M.; Zhu, C.; Chen, L.; Zhang, H.; Xia, H. *Chem. Sci.* **2016**, *7*, 1815–1818. (b) Zhou, X.; Wu, J.; Hao, Y.; Zhu, C.; Zhuo, Q.; Xia, H.; Zhu, J. *Chem. - Eur. J.* **2018**, *24*, 2389–2395.
- (a) Zhu, C.; Yang, Y.; Luo, M.; Yang, C.; Wu, J.; Chen, L.; Liu, G.; Wen, T. B.; Zhu, J.; Xia, H. *Angew. Chem., Int. Ed.* **2015**, *54*, 6181–6185. (b) Lu, Z.; Zhu, C.; Cai, Y.; Zhu, J.; Hua, Y.; Chen, Z.; Chen, J.; Xia, H. *Chem. - Eur. J.* **2017**, *23*, 6426–6431. (c) Zhu, C.; Zhu, J.; Zhou, X.; Zhu, Q.; Yang, Y.; Wen, T. B.; Xia, H. *Angew. Chem., Int. Ed.* **2018**, *57*, 3154–3157.
- (a) Cao, X.-Y.; Zhao, Q.; Lin, Z.; Xia, H. *Acc. Chem. Res.* **2014**, *47*, 341–354. (b) Fernandez, I.; Frenking, G.; Merino, G. *Chem. Soc. Rev.* **2015**, *44*, 6452–6463. (c) Frogley, B. J.; Wright, L. J. *Chem. - Eur. J.* **2018**, *24*, 2025–2038. (d) Wang, H.; Zhou, X.; Xia, H. *Chin. J.*

*Chem.* **2018**, *36*, 93–105. (e) Zhou, X.; Zhang, H. *Chem. - Eur. J.* **2018**, DOI: 10.1002/chem.201705679.

(17) Bond length ranges in this article are all based on a search of the *Cambridge Structural Database*, CSD, version 5.39; November 2017.

(18) (a) Cabioch, J.-L.; Dossett, S. J.; Hart, I. J.; Pilotti, M. U.; Stone, F. G. A. *J. Chem. Soc., Dalton Trans.* **1991**, 519–527. (b) Anderson, S.; Hill, A. F.; Nasir, B. A. *Organometallics* **1995**, *14*, 2987–2992.

(19) (a) Jeffrey, J. C.; Sambale, C.; Schmidt, M. F.; Stone, F. G. A. *Organometallics* **1982**, *1*, 1597–1604. (b) Carriedo, G. A.; Riera, V.; Sánchez, G.; Solans, X.; Labrador, M. *J. Organomet. Chem.* **1990**, *391*, 431–437.

(20) Brooner, R. E. M.; Widenhoefer, R. A. *Angew. Chem., Int. Ed.* **2013**, *52*, 11714–11724.

(21) (a) Dorel, R.; Echavarren, A. M. *Chem. Rev.* **2015**, *115*, 9028–9072. (b) Harris, R. J.; Widenhoefer, R. A. *Chem. Soc. Rev.* **2016**, *45*, 4533–4551.

(22) Selected references in which the  $[\text{Au}(\text{PR}_3)]^+$ -metal carbyne adducts were characterized by single-crystal X-ray diffraction: (a) Green, M.; Howard, J. A. K.; James, A. P.; Nunn, C. M.; Stone, F. G. A. *J. Chem. Soc., Dalton Trans.* **1987**, 61–72. (b) Goldberg, J. E.; Mullica, D. F.; Sappenfield, E. L.; Stone, F. G. A. *J. Chem. Soc., Dalton Trans.* **1992**, 2495–2502.

(23) (a) Bleeke, J. R.; Xie, Y. F.; Bass, L.; Chiang, M. Y. *J. Am. Chem. Soc.* **1991**, *113*, 4703–4704. (b) Bleeke, J. R.; Bass, L.; Xie, Y. F.; Chiang, M. Y. *J. Am. Chem. Soc.* **1992**, *114*, 4213–4219. (c) Bleeke, J. R.; Behm, R.; Xie, Y. F.; Chiang, M. Y.; Robinson, K. D.; Beatty, A. M. *Organometallics* **1997**, *16*, 606–623. (d) Jacob, V.; Landorf, C. W.; Zakharov, L. N.; Weakley, T. J. R.; Haley, M. M. *Organometallics* **2009**, *28*, 5183–5190.

(24) (a) Lee, C.; Yang, W.; Parr, R. G. *Phys. Rev. B: Condens. Matter Mater. Phys.* **1988**, *37*, 785. (b) Miehlisch, B.; Savin, A.; Stoll, H.; Preuss, H. *Chem. Phys. Lett.* **1989**, *157*, 200. (c) Becke, A. D. *J. Chem. Phys.* **1993**, *98*, 5648.

(25) Wiberg, K. B. *Tetrahedron* **1968**, *24*, 1083–1096.

(26) Hay, P. J.; Wadt, W. R. *J. Chem. Phys.* **1985**, *82*, 299.

(27) Huzinaga, S.; Andzelm, J.; Radzio-Andzelm, E.; Sakai, Y.; Tatewaki, H.; Klobukowski, M. *Gaussian Basis Sets for Molecular Calculations*; Elsevier Science Publishing: Amsterdam, 1984.

(28) Frisch, M. J.; Trucks, G. W.; Schlegel, H. B.; Scuseria, G. E.; Robb, M. A.; Cheeseman, J. R.; Scalmani, G.; Barone, V.; Mennucci, B.; Petersson, G. A.; Nakatsuji, H.; Caricato, M.; Li, X.; Hratchian, H. P.; Izmaylov, A. F.; Bloino, J.; Zheng, G.; Sonnenberg, J. L.; Hada, M.; Ehara, M.; Toyota, K.; Fukuda, R.; Hasegawa, J.; Ishida, M.; Nakajima, T.; Honda, Y.; Kitao, O.; Nakai, H.; Vreven, T.; Montgomery, J. A., Jr.; Peralta, J. E.; Ogliaro, F.; Bearpark, M.; Heyd, J. J.; Brothers, E.; Kudin, K. N.; Staroverov, V. N.; Kobayashi, R.; Normand, J.; Raghavachari, K.; Rendell, A.; Burant, J. C.; Iyengar, S. S.; Tomasi, J.; Cossi, M.; Rega, N.; Millam, J. M.; Klene, M.; Knox, J. E.; Cross, J. B.; Bakken, V.; Adamo, C.; Jaramillo, J.; Gomperts, R.; Stratmann, R. E.; Yazyev, O.; Austin, A. J.; Cammi, R.; Pomelli, C.; Ochterski, J. W.; Martin, R. L.; Morokuma, K.; Zakrzewski, V. G.; Voth, G. A.; Salvador, P.; Dannenberg, J. J.; Dapprich, S.; Daniels, A. D.; Farkas, O.; Foresman, J. B.; Ortiz, J. V.; Cioslowski, J.; Fox, D. J. *Gaussian 09*, revision D.01; Gaussian, Inc.: Wallingford, CT, 2009.

(29) Glendenning, E. D.; Badenhop, J. K.; Reed, A. E.; Carpenter, J. E.; Bohmann, J. A.; Morales, C. M.; Landis, C. R.; Weinhold, F. *NBO 6.0*; Theoretical Chemistry Institute, University of Wisconsin: Madison, WI, 2013.